Effects of tin and sulfur chemical substitution on the structural and electrical properties of $CuCr_2Se_4$ seleno-spinel

Paulina Valencia-Gálvez [1], Daniel Aravena [2], Patricia Barahona[3], Silvana Moris [4,*] and Antonio Galdámez [1,*]

[1] Departamento de Química, Facultad de Ciencias, Universidad+ de Chile, Las Palmeras 3425, Chile; paulygav@uchile.cl (P.V-G.)

[2] Departamento de Química de los Materiales, Facultad de Química y Biología, Universidad de Santiago de Chile, Casilla 40, Correo 33, Santiago 9170022, Chile; daniel.aravena.p@usach.cl (D. A.)

[3] Facultad de Ciencias Básicas, Universidad Católica del Maule, Talca, Chile (P.B.)

[4] Centro de Investigación de Estudios Avanzados del Maule (CIEAM), Vicerrectoría de Investigación y Postgrado, Universidad Católica del Maule, Avenida San Miguel 3605, Talca 3480112, Chile

* Correspondence: smoris@ucm.cl (S.M.); agaldamez@uchile.cl (A.G.)

Supplementary Materials

Table S1. Fractional atomic coordinates and isotropic or equivalent isotropic displacement parameters ($Å^2$)

	x	y	z	$U_{iso}*/U_{eq}$	Occ. (<1)
Cu	1/8	1/8	1/8	0.0174	
Sn	1/4	3/4	1/2	0.0034	0.435
Cr	1/4	3/4	1/2	0.0034	0.565
Se	0.25484	0.99516	0.49516	0.0066	0.432
S	0.25484	0.99516	0.49516	0.0066	0.568

* U_{eq} is defined as one third of the trace of the orthogonalized U_{ij} tensor. Cu in 8a site; Cr/ Sn in 16d site and S/Se in 32e site.

Table S2. Frequency and proposed mode assignment of Raman peaks.

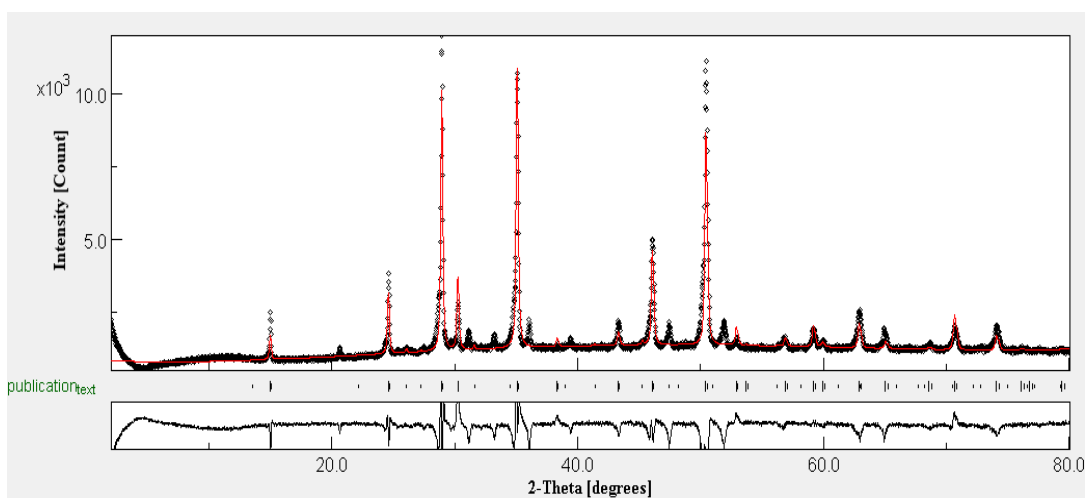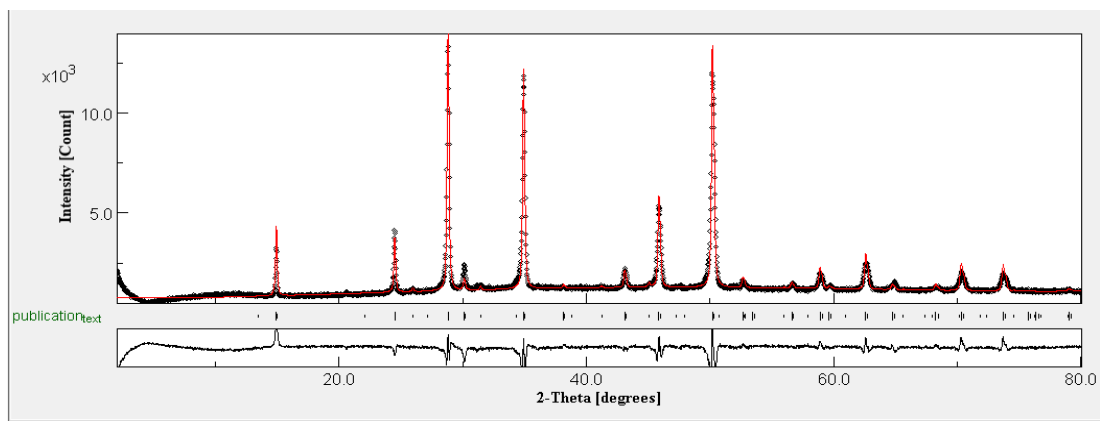| mode	$CuCrSnS_4$[7]	$CuCr_{1.6}Sn_{0.4}S_2Se_2$ [12]	$CuCrSnS_2Se_2$ [12]	*$CuCr_{1.6}Sn_{0.4}S_{2.3}Se_{1.7}$	*$CuCrSnS_{2.3}Se_{1.7}$
F_{2g} (1)	130	133	124	128	119
E_g	165	194	----	205	202
F_{2g} (2)	299	299	295	300	236
F_{2g} (3)	337	337	338	339	255
A_{1g}	379	382	---	382	335

*This work

Figure S1. Representative powder XRD data for $CuCr_{1.4}Sn_{0.6}S_{2.3}Se_{1.7}$ (top) and $CuCr_{1.6}Sn_{0.4}S_{2.3}Se_{1.7}$ (bottom) including profile fit, profile difference, and profile residuals from the corresponding Rietveld refinement using MAUD program. The intensities are plotted as the intensity *Q to show low-intensity reflections as well.
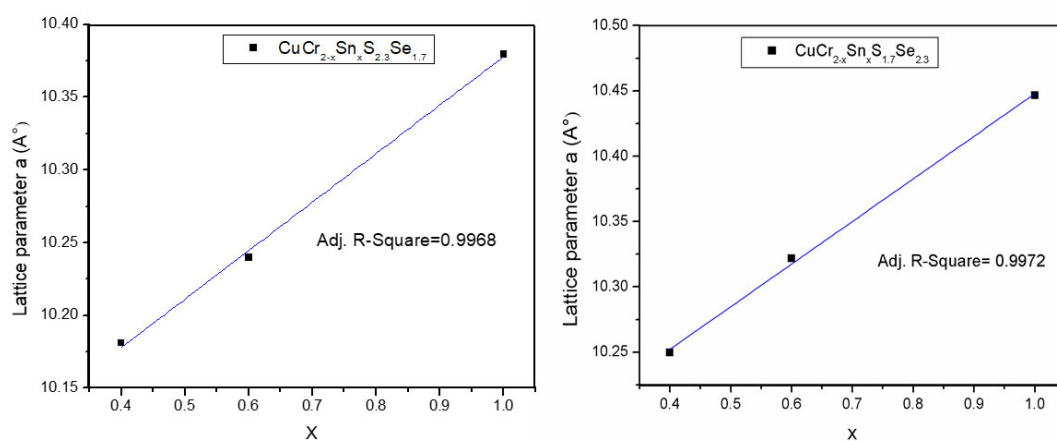

Figure S2. Vegard´s Law for $CuCr_{2-x}Sn_xS_{2.3}Se_{1.7}$ and $CuCr_{2-x}Sn_xS_{1.7}Se_{2.3}$ ($x = 0.4$; 0.6 y 1.0) phases.
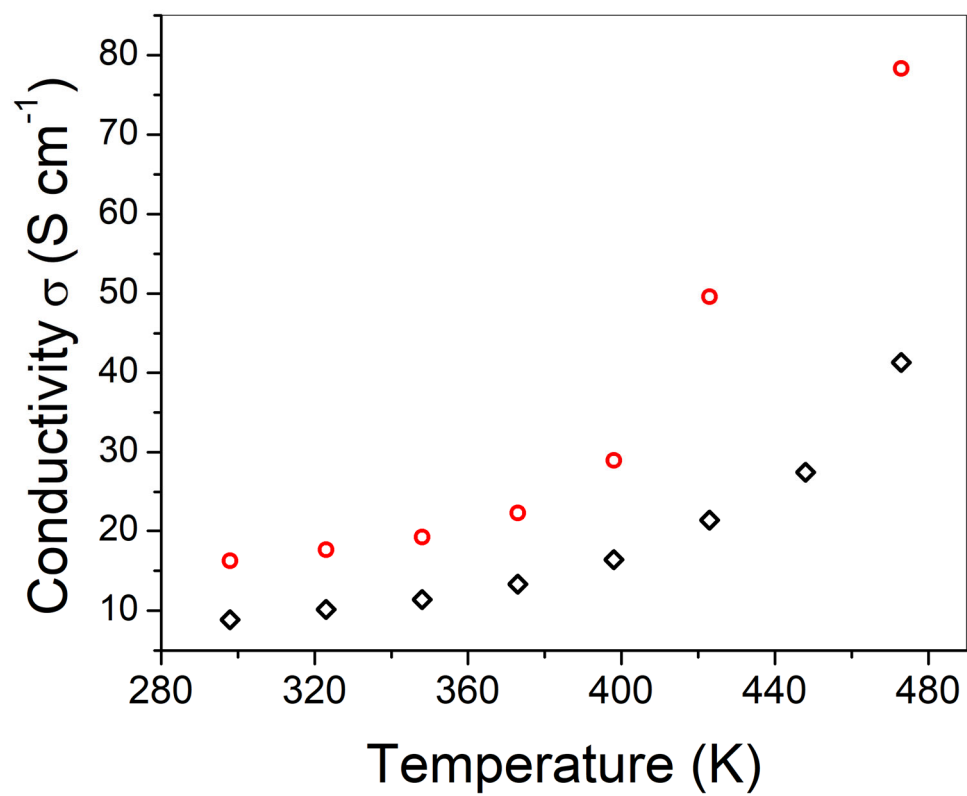
Figure S3. Electrical conductivity against Temperature of $CuCr_{2-x}Sn_xS_{2.3}Se_{1.7}$ x = 0.4 (red circles) and 0.6 (black diamonds) phases.
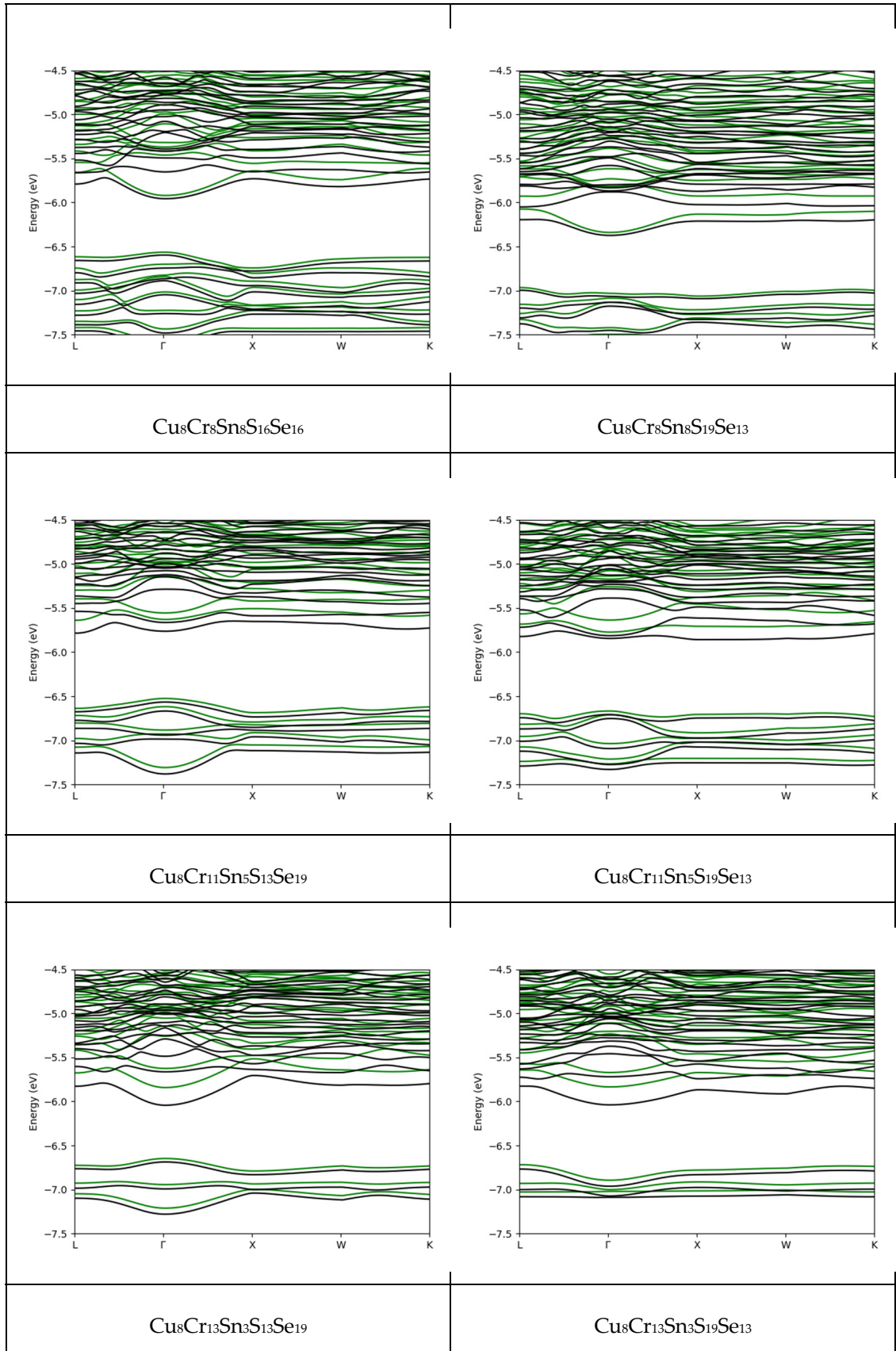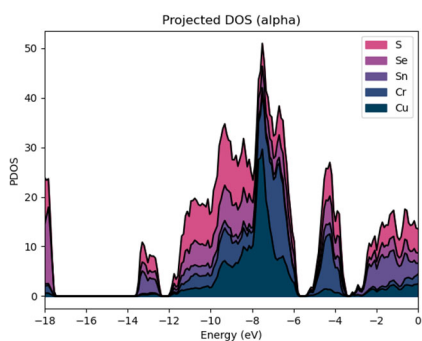
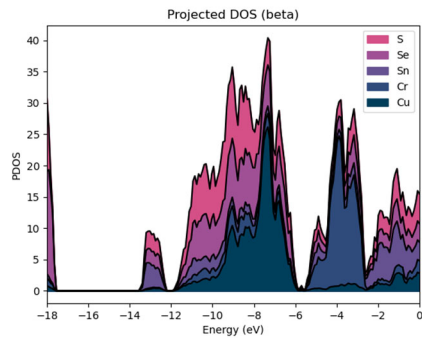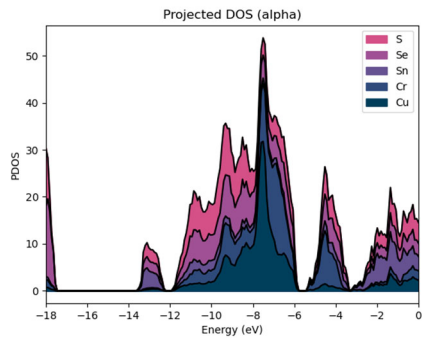**Figure S4.** Band structures for calculated models. Alpha bands are depicted in black and beta bands are presented in green.

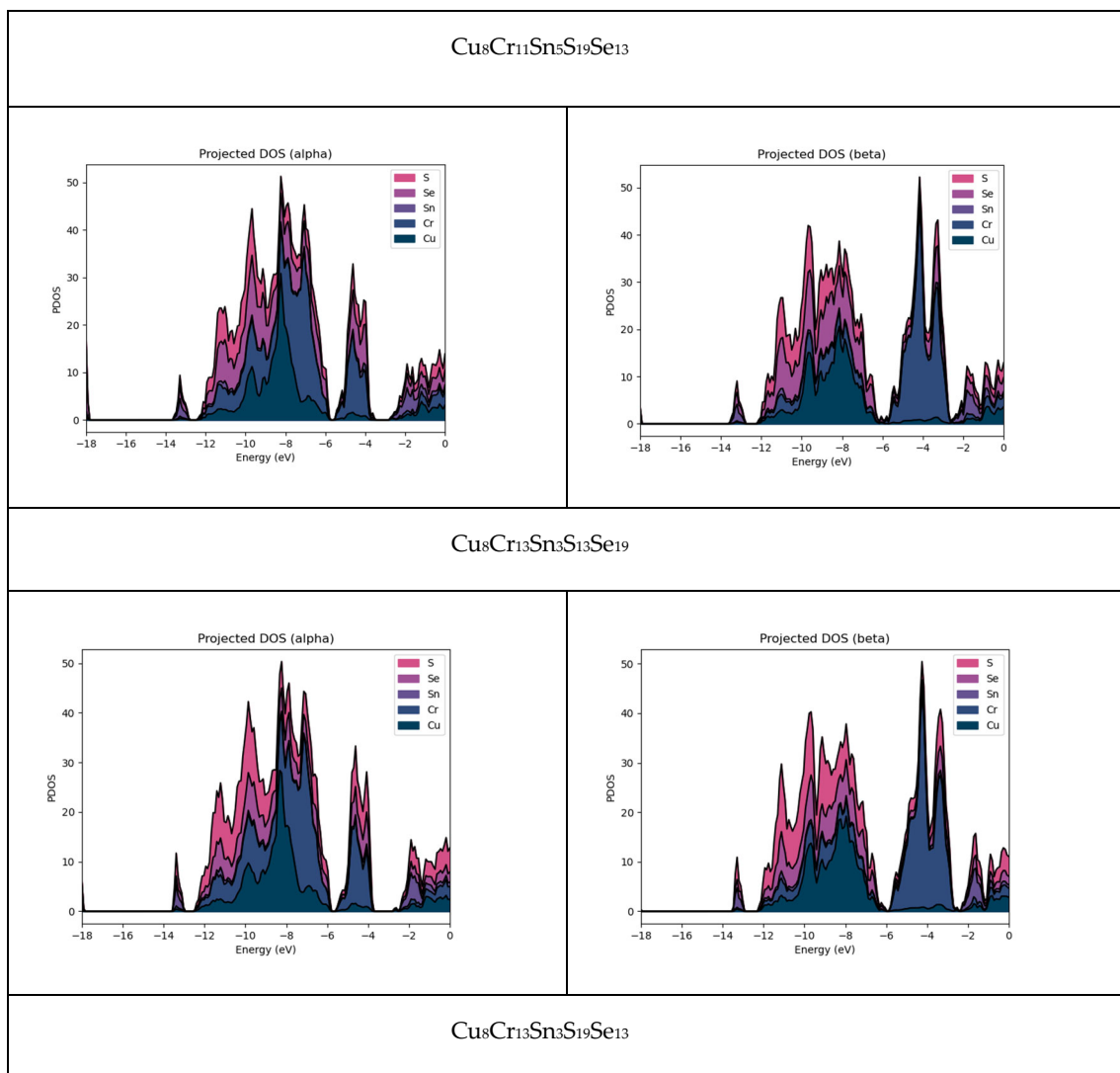Projected DOS (alpha) — Projected DOS (beta)

$Cu_8Cr_8Sn_8S_{16}Se_{16}$

Projected DOS (alpha) — Projected DOS (beta)

$Cu_8Cr_8Sn_8S_{19}Se_{13}$

Projected DOS (alpha) — Projected DOS (beta)

$Cu_8Cr_{11}Sn_5S_{13}Se_{19}$

Projected DOS (alpha) — Projected DOS (beta)

Cu₈Cr₁₁Sn₅S₁₉Se₁₃

$Cu_8Cr_{11}Sn_5S_{19}Se_{13}$

$Cu_8Cr_{13}Sn_3S_{13}Se_{19}$

$Cu_8Cr_{13}Sn_3S_{19}Se_{13}$
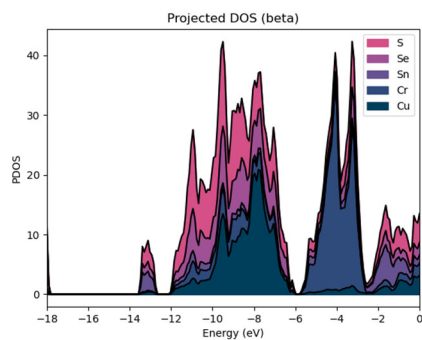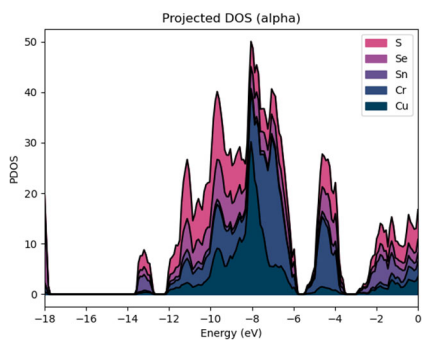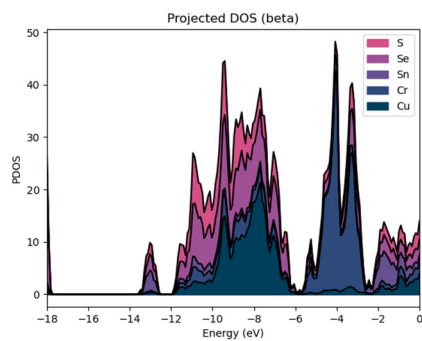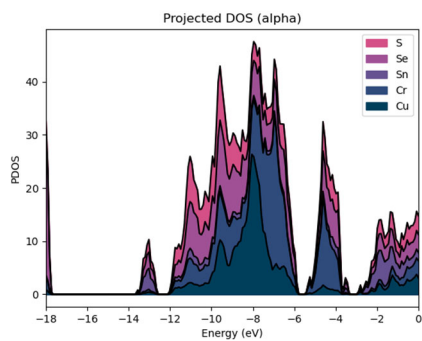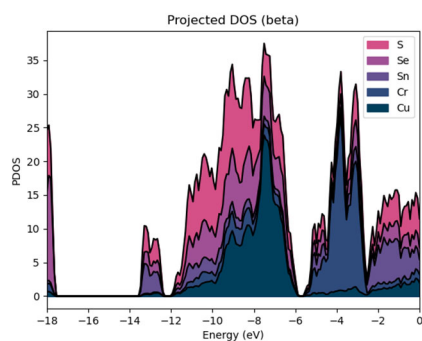
Figure S5 Element and spin resolved Density of states for all calculated systems.

Conflicts of Interest: The authors declare no conflicts of interest.